Deep-Sea Research I 79 (2013) 74–85

Contents lists available at SciVerse ScienceDirect

Deep-Sea Research I

journal homepage: www.elsevier.com/locate/dsri

High primary productivity and *f*-ratio in summer in the Ulleung basin of the East/Japan Sea

Jung Hyun Kwak [a], Jeomshik Hwang [a], Eun Jung Choy [b], Hyun Je Park [a], Dong-Jin Kang [c], Tongsup Lee [d], Kyung-Il Chang [e], Kyung-Ryul Kim [e], Chang-Keun Kang [a,*]

[a] POSTECH Ocean Science & Technology Institute, Pohang University of Science and Technology, Pohang 790-784, South Korea
[b] Korea Polar Research Institute, Korea Ocean Research and Development Institute (KORDI), Incheon 406-840, South Korea
[c] Marine Instrument Service and Calibration Department, KORDI, P.O. Box 29, Ansan 425-600, South Korea
[d] Department of Ocean System Science, Pusan National University, Busan 609-735, South Korea
[e] School of Earth and Environmental Sciences/Research Institute of Oceanography, Seoul National University, Seoul 151-747, South Korea

ARTICLE INFO

Article history:
Received 2 September 2012
Received in revised form
12 May 2013
Accepted 16 May 2013
Available online 6 June 2013

Keywords:
Primary productivity
Nitrogen uptake
f-ratio
Hydrography
Nitrate upward flux
East/Japan Sea

ABSTRACT

To better understand the cause of high summer primary productivity in the Ulleung Basin located in the southwest part of the East/Japan Sea, the spatial dynamics of primary, new, and regenerated productivities (PP, NP, and RP) were examined along the path of the Tsushima Warm Current system in summer 2008. We compared hydrographic and chemical parameters in the Ulleung Basin with those of the Kuroshio Current in the Western Pacific Ocean and the East China Sea. In summer, integrated primary productivity (IPP, 0.37–0.96 g C m^{-2} d^{-1}) and integrated new productivity (INP, 26–221 mg N m^{-2} d^{-1}) within the euphotic zone in the Ulleung Basin were higher than those in the East China Sea and the Western Pacific Ocean (0.17–0.28 g C m^{-2} d^{-1}, 2–5 mg N m^{-2} d^{-1}, respectively). In contrast, there was no pronounced spatial variation in integrated regenerated productivity (IRP, 43–824 mg N m^{-2} d^{-1}). Strong positive correlations between IPP and INP (also the *f*-ratio), and between nitrate uptake rate in the mixed layer and nitrate upward flux through the top of pycnocline in summer in the Ulleung Basin imply that the high IPP was mainly supported by supply of nitrate from the underlying water in the euphotic zone. Shallowing of the pycnocline depth as the current enters the East/Japan Sea facilitates nitrate supply from the nutrient-replete cold water immediately below the pycnocline through nitrate upward flux. A subsurface maximum in PP at or above the pycnocline and a high *f*-ratio further support the importance of this source of nitrate for maintaining the high summer PP in the Ulleung Basin. In comparison, the high PP layer was observed at the surface in the following fall and spring in the Ulleung Basin. Our results demonstrate the importance of hydrographic features in enhancing PP in this oligotrophic Tsushima Warm Current system.

1. Introduction

The East/Japan Sea (hereafter, the EJS), located in the northwestern Pacific Ocean, is a marginal sea with an area of 1.01×10^6 km^2 (Fig. 1). Of the three major deep basins (the Ulleung, Yamato, and Japan basins), the Ulleung Basin (UB) is located in the southwest of the EJS. The prevailing surface current in the UB is the Tsushima Warm Current (TWC), which branches off the Kuroshio Current, a warm and saline western boundary current of the Western Pacific Ocean (WPO). The TWC flows northward through the East China Sea (ECS) and enters the EJS through the Korea/Tsushima Strait. Upon entering the UB, the TWC flows over the cold East/Japan Sea Proper Water (ESPW) (Chang et al., 2004). Despite the prevalence of the nutrient-poor surface water mass of the TWC, primary production in the southwest EJS (i.e. the UB) is relatively high compared with that in the Yamato and Japan basins within the EJS and the adjacent seas (Yamada et al., 2005; Hyun et al., 2009; Yoo and Park., 2009).

Primary production in the temperate oceans shows seasonality mainly caused by seasonal dynamics of physical factors including variations of light, wind, vertical mixing, and stratification, and thereby varying nutrient concentrations in the euphotic zone (Howarth et al., 1988; Marty et al., 2008). The importance of nitrate supply into the euphotic zone in regulating primary production has been demonstrated in many cases in the ocean, where seasonal stratification is a dominant feature (Eppley et al., 1979; Vitousek and Howarth, 1991). Based on the source and species of nitrogen (N), primary production is operationally

* Corresponding author. Tel.: +82 54 279 9501; fax: +82 54 279 9519.
E-mail address: ckkang@postech.ac.kr (C.-K. Kang).

0967-0637/$ - see front matter © 2013 Elsevier Ltd. All rights reserved.
http://dx.doi.org/10.1016/j.dsr.2013.05.011

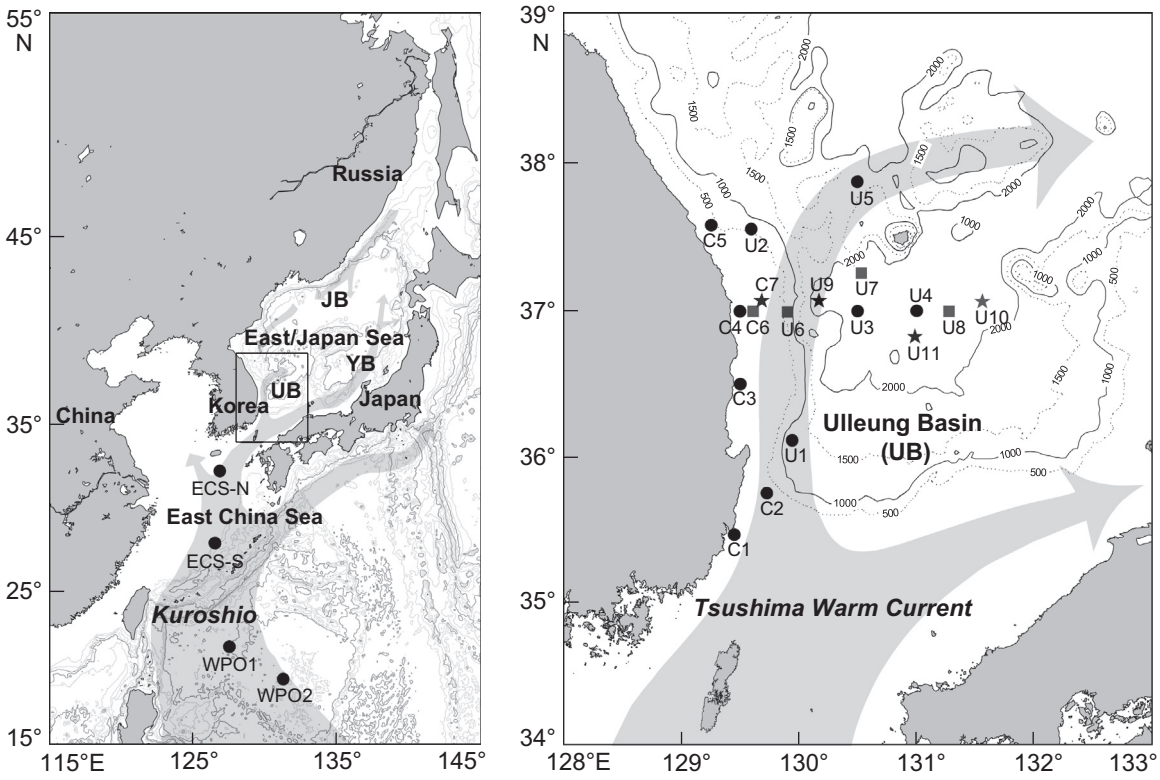

Fig. 1. Overview of the study region. The circles, squares and stars indicate sampling stations in summer, fall and spring, respectively. The shaded arrows indicate major currents of the study area.

partitioned into new production and regenerated production (Dugdale and Goering, 1967). New production is defined as the portion of primary production that utilizes N supplied from outside the euphotic zone. The N sources include nitrate (NO_3^-) supplied from the deeper layer by vertical mixing, and other N species transported via river discharges, atmospheric deposition, and biological N_2 fixation (Chen et al., 1999). Among these sources, nitrate supplied by vertical mixing has been known to be the dominant inorganic species in the oceanic environment (Dugdale et al., 1992). Regenerated production is the portion of primary production that utilizes regenerated N, mainly in the form of ammonium (NH_4^+) and urea, that derives from the metabolic products of biological processes within the euphotic zone. In summer, nitrate-based new production is restrained because the development of stratification limits nutrient supply, thus primary production is mainly supported by ammonium-based regenerated production and is generally low in temperate oceans (Dugdale and Goering, 1967; Bode et al., 2002). Therefore, if nitrate is supplied to the euphotic zone, a high rate of nitrate uptake may enhance primary productivity even in a well-stratified oceanic environment (Eppley et al., 1979; Metzler et al., 1997; L'Helguen et al., 2002).

Curiously, primary production in summer in the UB has been observed to be high. Therefore, the UB is an abnormal case that does not follow the dogmatic Sverdrup theory for the seasonality of primary production (Sverdrup, 1953). There are several examples that have dealt with a mechanism of such an abnormal event in the North Pacific Subtropical Gyre where summer blooms were observed (Dore et al., 2008; Wilson et al., 2008). However, the cause for this abnormality in the UB is not well understood. Revealing the mechanism responsible for the high PP in summer may further our understanding on one of the most important biological parameters. Also, continued high PP in summer may indicate high biological pump efficiency for CO_2-sequestration. Several studies attemped to explain the cause of the unexpectedly high PP, including coastal upwelling (Hyun et al., 2009; Yoo and Park., 2009). Upwelling of nutrient-rich subsurface water on the southeast coast of the Korean peninsula occurs when S–SW wind blows along the coast during the summer monsoon (Lee, 1983; Lee and Na, 1985). The hypothesis is that once upwelling brings nutrient-replete water to the surface near the coast, the East Korean Warm Current, a branch of the TWC, transports the nutrient-rich coastal water into the central UB expanding the area of high primary productivity (Isoda and Saitoh, 1993; Chang et al., 2004; Shin et al., 2005). However, the upwelling events occur episodically during a short duration. Furthermore, satellite images showed that the cold water from the upwelling formed a narrow stream (cf. Hyun et al., 2009; Yoo and Park., 2009), thus the affected area might be rather limited. Therefore, there may be another mechanism to cause the high primary productivity observed in the broad area of the UB in addition to coastal upwelling.

In order to better understand the mechanism responsible for maintaining high primary productivity in summer in the UB, we examined the spatial variability of various hydrographic and chemical parameters in the UB and compared them to those of the WPO and the ECS that belong to the same TWC system. Additionally for temporal comparison, we also examined primary production and the related hydrographic features in the UB for the following fall and spring.

2. Materials and methods

2.1. Study sites

Two field campaigns were carried out along the pathway of the TWC from the Kuroshio Current in the west Pacific through the

ECS to the EJS: one during the early summer (2–25 June 2008) in the WPO and the ECS, aboard R/V Onnuri, and the other during the middle of summer (6–14 August 2008) in the EJS aboard R/V Haeyang 2000 (Fig. 1). A total of 14 stations were occupied during these cruises. Stations WPO1 and WPO2 were in the warm pool in the WPO. Stations ECS-N and ECS-S were in the ECS where the TWC branches off the Kuroshio Current. Stations C1–C5 were on the continental shelf (<250 m deep) off the east coast of the Korean peninsula. Station C1 was representative of an upwelling site, and Stations U1–U5 were in the UB. In order to examine the seasonal variability in the UB, two more campaigns were carried out in the following fall (28 October–8 November 2008) and spring (11–15 May 2009) aboard R/V Eardo and R/V Tamyang, respectively. Four stations were occupied on an east–west transect crossing the UB (Stations C6, U6, U7, and U8 in spring and Stations C7, U9, U10, and U11 in fall).

2.2. Sampling

Water samples for total carbon dioxide (TCO_2) for determination of carbon uptake rate, nutrient analyses, and biochemical measurements were collected from six depths corresponding to 100%, 50%, 30%, 15%, 5%, and 1% of surface irradiance, using a CTD-rosette system equipped with 10 L Niskin bottles. Temperature and salinity were measured using a CTD (SBE 911 Plus, Seabird Electronics Inc., Bellevue, USA), and irradiance was measured using a PAR sensor (OSP200L, Biospherical Inc., San Diego, CA) between surface and the depth of the euphotic zone (designated in this study as the depth at which light intensity was 1% of surface irradiance). Light intensity was also measured on board to determine the daily irradiance and experimental conditions using a PAR sensor (Li-1400, Li-cor Inc., Lincoln, USA). Water samples for nutrient analysis were filtered through pre-combusted (at 450 °C for 2 h) Whatman GF/F filters, immediately transferred into acid-washed polyethylene bottles, and stored frozen at −20 °C until analysis in the land-based laboratory. Approximately 1 L and 500 mL of water samples for chlorophyll *a*, and particulate organic carbon (POC) and nitrogen (PON) analyses, respectively, were gently filtered onto 25 mm pre-combusted (450 °C, 2 h) Whatman GF/F filters after pre-filtration through 200 μm Nytex net. Upon visual inspection, no large phytoplankton colonies or chains were detained on the screen. The filters were kept frozen at −20 °C until analysis.

2.3. Onboard sample treatment for determination of carbon and nitrogen uptake rates

TCO_2 was determined onboard by single-point addition of HCl (0.01 N) and pH measurement before and after the acid addition (Edmond and Gieskes, 1970). Water samples for carbon and nitrogen uptake measurements were pre-filtered through 200 μm Nytex net and dispensed into two sets of acid-washed, transparent polycarbonate bottles (Nalgene, 1 L). For determination of primary productivity by carbon uptake rate, $NaH^{13}CO_3$ (98 atom %, Isotec, Sigma-Aldrich, Miamisburg, OH, USA) solution was added to each sample to a resulting concentration of 0.2 mM, corresponding to about 10% of the ambient concentrations. $Na^{15}NO_3$ (98 atom %, Isotec) and $^{15}NH_4Cl$ (98 atom %, Isotec) were added to each sample for determination of new and regenerated productivities, respectively, to resultant concentrations equivalent to about 10% of the ambient nitrate and ammonium concentrations. The minimum nitrate and ammonium concentrations were 0.09 μM and 0.05 μM, respectively. The uncertainties in measurements of nitrogen uptake rates are known to increase as the ambient nutrient concentrations become low because addition of dissolved ^{15}N in nitrogen-poor water enhances N-uptake, resulting in the overestimation of uptake rate (L'Helguen et al., 2002). The amounts of ^{15}N to be added were decided based on numerous nitrate and ammonium concentration data previously measured in the study area, so that, in most cases, the added amounts were less than 10% of the ambient concentrations. However, in a few cases where ammonium concentrations were very low, addition of minimum amount of ^{15}N resulted in up to about 50% of the ambient concentrations. The bottles were covered with calibrated layers of neutral density screen to adjust the irradiance to be equivalent to those at the six depths where the water samples were collected. The water samples were incubated on deck under natural light for three to four hours (from 8 to 9 a.m. to noon) in order to minimize isotope dilution effects due to nitrogen recycling (Glibert et al., 1982b; Kanda et al., 1987; Peña et al., 1992). Incubation temperature was controlled to be similar to in situ temperature by running surface seawater for the samples from the upper three depths and by a cooling system for the samples from the lower three depths. At the termination of the incubation, the waters were filtered through pre-combusted (450 °C, 2 h) Whatman GF/F filters under a low vacuum of about 100 mm Hg. The sample filters were stored at −20 °C until laboratory analyses. More detail on the experimental procedures is given in Hama et al. (1983) and Dugdale and Wilkerson (1986).

2.4. Laboratory analyses

Dissolved inorganic nitrogen species (nitrate, nitrite, and ammonium) were determined by standard spectrophotometric methods (Parsons et al., 1984). Chlorophyll *a* was extracted with 90% acetone in the dark at 4 °C for 20 h, and was determined fluorometrically using a Turner Designs fluorometer (Sunnyvale, CA) (Parsons et al., 1984), with a precision (SD) of ± 0.05 μg L^{-1}. The filtered samples, for measurements of POC, PON and the ^{13}C and ^{15}N isotope ratios, were fumed with HCl for 12 h to remove carbonate and were subsequently freeze-dried. The dried samples were analyzed with a CHN elemental analyzer (Eurovector 3000 Series, Milan, Italy) coupled with a continuous-flow isotope ratio mass spectrometer (IsoPrime, GV Instruments, Manchester, UK). The uncertainties for $\delta^{13}C$ and $\delta^{15}N$ measurements were ± 0.1‰ and ± 0.3‰, respectively. Every sample was analyzed in duplicate and mean values are reported.

2.5. Calculation of carbon and nitrogen uptake rates and nitrate upward flux

Carbon and nitrogen (nitrate and ammonium) uptake rates were calculated following Hama et al. (1983) and Dugdale and Wilkerson (1986), respectively. Ammonium uptake rates were not corrected for isotope dilution because the incubation time was short and errors due to isotope dilution by ammonium recycling in oceanic samples are reported to be small (Kanda et al., 1987; Peña et al., 1992). Only daytime uptake values were used to calculate daily nitrogen uptake rates because of a lack of nighttime data. Daily primary productivity and nitrate uptake rates were estimated by multiplying measured C and N uptake rates by photoperiod conversion factors (Kanda et al., 1985; Fan and Glibert, 2005) (the ratios of daily total irradiance to integrated irradiance during incubation). Finally, daily nitrate uptake rates and daily ammonium uptake rates were corrected to correspond to 12 h, and 18 h periods, respectively, to reflect that ammonium uptake is less light-dependent than nitrate uptake (McCarthy et al. 1996). Details of this correction are described in Parker et al. (2011). Depth-integrated uptake rates were calculated by trapezoidal integration of the entire euphotic zone (1–100% of surface irradiance) and reported as g C m^{-2} d^{-1} and g N m^{-2} d^{-1}. The *f*-ratio was calculated as a fraction of nitrate uptake to the sum of nitrate and ammonium uptake (Eppley and Peterson, 1979).

We estimated the nitrate upward flux through the bottom of the mixed layer as representing the nitrate supply from the underlying water (King and Devol, 1979). The nitrate upward flux (F_n, μmol NO_3 m^{-2} h^{-1}) was a product of the vertical nitrate

gradient ($\Delta NO_3^-/\Delta Z$, mmol m^{-4}) and the coefficient of vertical eddy diffusivity (K_Z, $cm^2\ s^{-1}$). We adopted the same K_Z values estimated from an empirical equation determined by density gradients and nitrate gradients below the mixed layer (King and Devol, 1979) in eastern tropical Pacific water, as follows: $K_Z\ (cm^2\ s^{-1}) = 643.0 \times (10^6E)^{-1.61}$, where 10^6E was the unit of stability with depth (Z) in meters.

3. Results

3.1. Spatial variability in the TWC system

Vertical profiles of density (σ_t) exhibited marked spatial variation in vertical stratification and pycnocline depths (Fig. 2). Along the pathway of the TWC from the WPO to the EJS, pycnocline depth was observed to become shallower. Density changed gradually with depth and hence pycnoclines did not form clearly at the stations in the WPO and at Station ECS-S. In contrast, ECS-N and the stations in the EJS were characterized by stronger stratification, with the pycnocline depths being shallower than 250 m. Stations in the EJS were distinct from those in the WPO and the ECS: with the exception of Station C1, a thin layer of low-salinity and high-temperature water overlay the top 10 m of the water column, resulting in strong stratification at about 10 m depth. The mixed layer depth, defined such that the density (σ_t) gradient between the surface and this depth exceeded 0.1 m^{-1} (Chen et al., 2001), was extremely shallow (< 10 m) in the SW EJS. The stability index, calculated as the ratio of difference in σ_t between the surface and bottom of the euphotic zone to the thickness of the euphotic zone (Cho et al., 2001), in the EJS was higher (Mann-Whitney U test, $p = 0.005$., using SPSS 12.0) than

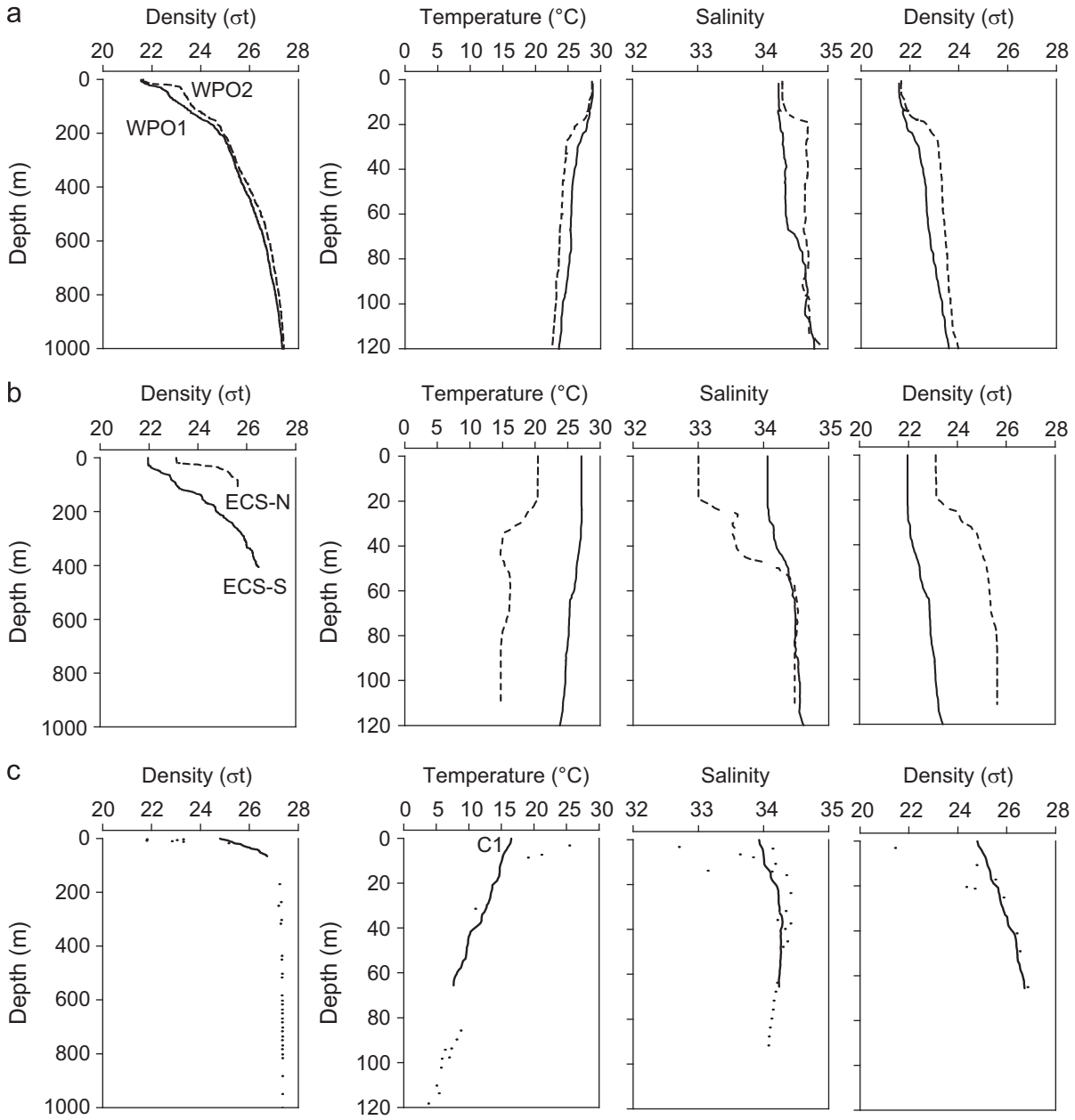

Fig. 2. Vertical profiles of density (σ_t), temperature, and salinity at stations located (a) in the WPO, (b) in the ECS, (c) in the UB. Legends for individual profiles in (c) are not provided with the exception of the C1 station (solid line) in the UB. (a) Western Pacific Ocean, (b) East China Sea and (c)Ulleung Basin (East/Japan Sea).

Table 1
Spatial and seasonal variations of the mixed layer depth (Z_{ML}), the euphotic depth (ZE), the stability index and depth-integrated values for nitrate, chlorophyll *a* (Chl. *a*), primary production (IPP), new production (INP), regenerated production (IRP), *f*-ratio, and IPP_{ML}:IPP ratio (IPP_{ML}/IPP) in the euphotic zone.

Season	Site	Depth (m)	Z_{ML} (m)	ZE (m)	Stability index	ΣNO_3 (mmol m^{-2})	Chl. *a* (mg m^{-2})	IPP (g C m^{-2} d^{-1})	INP (mg N m^{-2} d^{-1})	IRP (mg N m^{-2} d^{-1})	*f*-Ratio	IPP_{ML}/IPP
Summer	WPO1	4887	13	95	0.017	26	16	0.23	2	43	0.04	0.12
	WPO2	5500	17	115	0.019	68	36	0.17	4	160	0.03	0.16
	ECS-S	605	63	80	0.012	38	49	0.28	5	164	0.03	0.33
	ECS-N	117	20	55	0.039	221	21	0.28	5	89	0.06	0.51
	C1	70	2	13	0.042	91	120	2.41	1051	131	0.89	0.24
	C2	240	3	43	0.100	603	59	1.59	804	397	0.67	0.23
	C3	105	3	32	0.170	302	91	0.97	151	193	0.44	0.10
	C4	133	3	46	0.082	482	46	0.45	74	90	0.45	0.20
	C5	242	5	54	0.083	321	157	1.70	606	824	0.42	0.14
	U1	1365	8	43	0.082	444	45	0.96	221	288	0.43	0.19
	U2	756	5	54	0.074	361	84	0.71	203	434	0.32	0.11
	U3	2171	8	57	0.076	175	30	0.54	112	197	0.36	0.11
	U4	2156	9	46	0.071	491	50	0.37	26	136	0.16	0.11
	U5	1652	4	57	0.079	187	53	0.44	74	127	0.37	0.16
Fall	C6	133	5	16	0.029	37	11	0.45	74	86	0.46	0.39
	U6	1054	30	60	0.030	585	10	0.39	14	68	0.17	0.70
	U7	2167	46	50	0.018	320	15	0.38	17	128	0.12	0.97
	U8	2156	39	60	0.026	361	14	0.40	8	69	0.11	0.78
Spring	C7	218	8	16	0.026	358	29	0.49	166	50	0.77	0.63
	U9	2200	22	32	0.011	337	24	0.83	242	80	0.75	0.88
	U10	2166	22	32	0.012	212	26	0.61	80	222	0.27	0.79
	U11	2053	17	38	0.013	299	21	0.94	156	90	0.63	0.68

those in the ECS and the WPO (Table 1). Coastal upwelling is known to occur in the region near Station C1 (Yoo and Park, 2009), and the station seemed to be affected by upwelling during the study period. At this station, temperature (salinity) decreased (increased) gradually with increasing depth.

Vertical distribution of nitrate showed considerable spatial variation (Fig. 3). In the figures, we only presented the results of representative stations: WPO1 for WPO, ECS-S for ECS, C1 for an upwelling station, C3 for coastal stations in the UB, and U3 for offshore stations in the UB (see Appendix A for the complete results). At Station ECS-N and the EJS stations (Fig. 3), nitrate concentration increased sharply with increasing water depth below the mixed layer, from 0.0–3.7 μM within the mixed layer to 0.5–21.3 μM below the mixed layer. In contrast, at Stations ECS-S, WPO1 and WPO2, nitrate concentration was low (0.11–0.80 and 0.02–0.40 μM, respectively) within the euphotic zone. Nitrate standing stock (ΣNO_3) in the euphotic zone was 16–68 mmol m^{-2} in the WPO, 38–221 mmol m^{-2} in the ECS, and 91–603 mmol m^{-2} in the EJS (Table 1). Ammonium concentrations showed no significant variation either with depth or among sampling sites. The ammonium concentration in the euphotic zone ranged from 0.0 to 1.4 μM (average $\pm$ S.D. $= 0.4 \pm 0.3$ μM). Further discussion on the detailed profile data was not introduced here.

Concentration and vertical distributions of chlorophyll *a* varied spatially as well (Fig. 3b). The summer chlorophyll *a* concentration was lower than 0.7 μg L^{-1} near the surface with the exception of the upwelling-influenced Station C1 (~4.0 μg L^{-1}). In the EJS, the subsurface chlorophyll *a* maximum (SCM, 1.2–4.8 μg L^{-1}) layer was pronounced near the nitracline. In contrast, the SCM was not clearly observed in the ECS and the WPO. Chlorophyll *a* concentrations at these stations were low (0.8 and 0.5 μg L^{-1}, respectively) and showed small vertical variation. Depth-integrated chlorophyll *a* standing stock over the euphotic zone was much higher in the EJS (30–157 mg m^{-2}) than those in the WPO and the ECS (21–49 and 16–36 mg m^{-2}, respectively).

Primary productivity (PP) determined by carbon uptake rate was consistently higher in the EJS than that in the ECS and the WPO (Fig. 3c). The maximum PP in the ECS and the WPO was observed near the surface, and the values immediately below the surface were small and uniform with depth. In contrast, at most stations in the EJS, the maximum PP was observed at depths corresponding to the nitracline and the SCM. PP in the mixed layer was considerable, although chlorophyll *a* concentration was very low. The highest PP, up to 290 mg C m^{-3} d^{-1}, was observed at the surface of Station C1. Depth-integrated PP over the euphotic zone (IPP) was considerably higher at the EJS stations than at the ECS and the WPO stations. The proportion of integrated PP in the surface mixed layer (IPP_{ML}) in IPP was generally low (Table 1).

Vertical distributions of new productivity (NP) determined by nitrate uptake rate were similar to those of PP (Fig. 3d). NP values were significantly higher (Mann-Whitney *U* test, $p < 0.001$) in the EJS than in the ECS and the WPO. The highest NP values, up to 100 mg N m^{-3} d^{-1}, were observed at Station C1. NP within the mixed layer in the EJS was low but considerable compared to that in the ECS and the WPO. The maximum NP at each station was observed at the depth where the PP was maximal in the EJS, whereas NP was nearly undetectable over the entire euphotic zone in the ECS and the WPO. Depth-integrated NP (INP) over the euphotic zone varied from 2–5 mg N m^{-2} d^{-1} in the ECS and the WPO to 26–1051 mg N m^{-2} d^{-1} in the EJS, showing large spatial variability. Regenerated productivity (RP) determined by ammonium uptake rate was comparable to NP in the EJS, but was higher than NP in the WPO and at ECS-S. Although the RP at the SCM layer was significantly higher in the EJS than in the ECS and the WPO (Mann-Whitney *U* test, $p < 0.001$), depth-integrated RP (IRP, 43–824 mg N m^{-2} d^{-1}) over the euphotic zone did not exhibit any significant spatial difference (Kruskal-Wallis ANOVA, $p = 0.065$). The *f*-ratios, [INP/(INP+IRP)], in the euphotic zone varied greatly between 0 and 1. The values were higher in the EJS (0.16–0.89) than in the ECS and the WPO (0.03–0.06) (Table 1).

3.2. Seasonal variability in the EJS

The temperature in the surface water decreased from > 23.3 °C in summer (with the exception of Station C1) to < 20.9 °C in fall

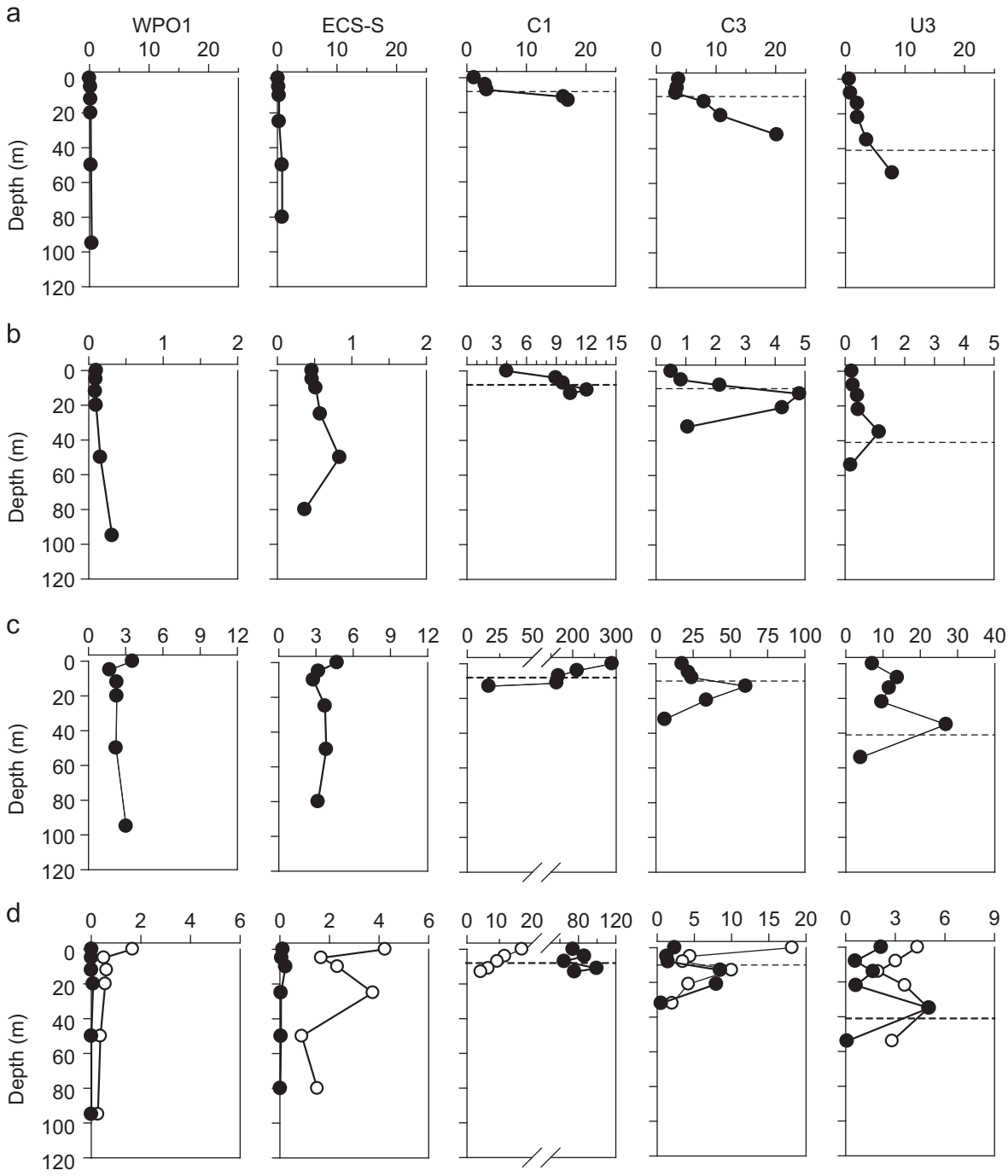

Fig. 3. Vertical profiles of (a) nitrate, (b) chlorophyll *a* concentration, (c) primary productivity (PP), (d) new productivity (NP, closed circles) and regenerated productivity (RP, open circles) in summer at each representative station, WPO1, ECS-S, C1, C3 and U3. Horizontal dashed lines represent the nitracline where nitrate concentration increased above 5 μM.

and < 16.8 °C in the following spring. The mixed layer became thicker (30–40 m) in fall, although the water column was still well stratified (Fig. 4a). By the following spring, the pycnocline became unclear (Fig. 4b). A slight increase in nitrate concentration (> 1.49 μM) in surface water was observed in fall at the basin stations of the EJS (Fig. 5a). Nitrate concentration increased with increasing depth from the surface in spring, whereas nitrate concentration increased sharply at below the mixed layer in summer.

Chlorophyll *a* concentration was generally low (< 0.5 μg L^{-1}) in fall (Fig. 5b). The maximum chlorophyll *a* concentration of 1.1 μg L^{-1} was observed at the SCM depth at Station C6. In spring, chlorophyll *a* concentration was higher than that in fall and the SCM was developed at Station C7. Depth-integrated chlorophyll *a* in the euphotic zone was slightly lower in fall (11–15 mg m^{-2}) than in spring (21–29 mg m^{-2}) (Table 1).

Primary productivity ranged between 2.8 and 43 mg C m^{-3} d^{-1} in fall and between 1.0 and 58 mg C m^{-3} d^{-1} in spring (Fig. 5c). Vertical profiles of PP in fall and spring were different from those in summer: PP was highest at the surface and decreased sharply with increasing depth. IPP in the UB (Stations U1–U11 in Table 1) were 0.37–0.96, 0.39–0.45, and 0.49–0.94 g C m^{-2} d^{-1} in summer, fall, and spring, respectively (Table 1), exhibiting no significant seasonal variation (Kruskal–Wallis test, $p=0.110$).

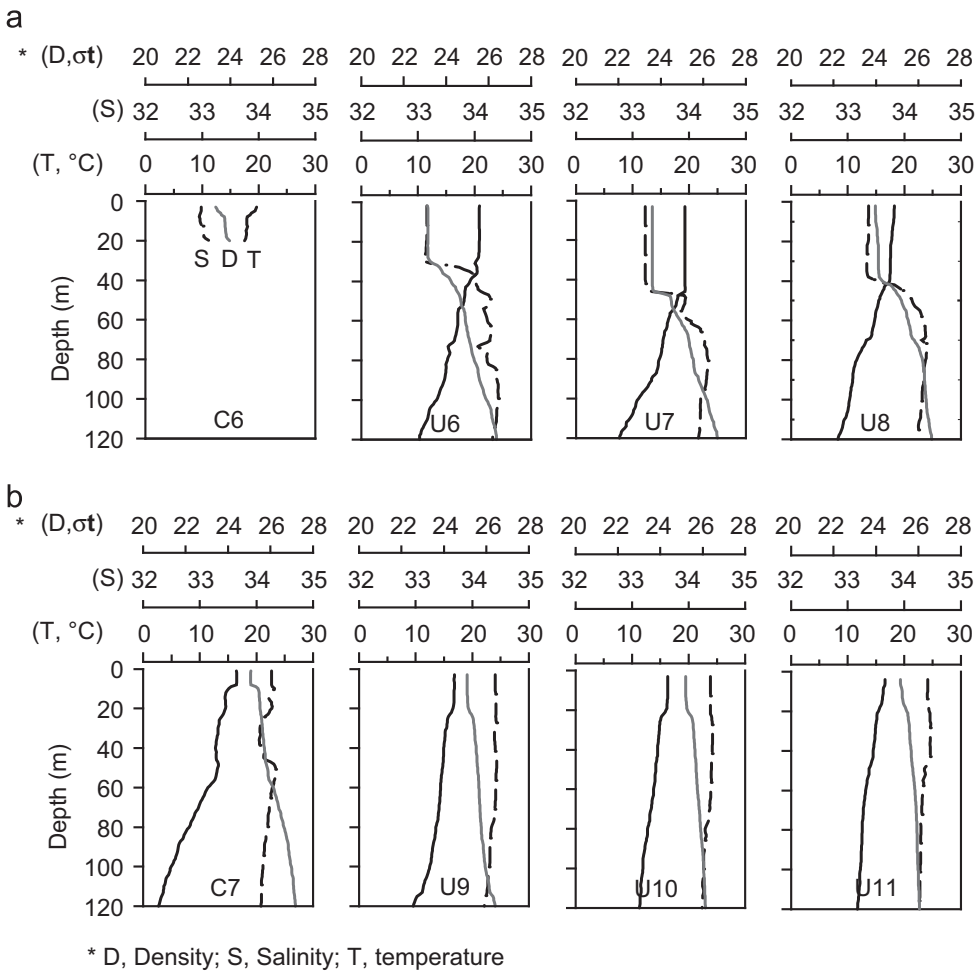

Fig. 4. Vertical profiles of salinity, temperature, and sigma-t (a) in fall and (b) in spring at selected stations in the UB.

NP in the UB in fall was nearly constant with depth and generally low ($<$ 1.0 mg N m^{-2} d^{-1}). NP in spring (1.6–8.7 mg N m^{-3} d^{-1}) was slightly higher than that in fall (0.1–5.1 mg N m^{-3} d^{-1}). There was no clear tendency in vertical distribution (Fig. 5d). INP in the UB was 26–221, 8–74, and 80–242 mg N m^{-2} d^{-1} in summer, fall, and spring, respectively (Table 1), exhibiting significant seasonal variation (Kruskal-Wallis test, $p=0.043$). RP in the UB ranged from 0.06 to 9.0 and from 0.81 to 15 mg N m^{-3} d^{-1} in fall and spring, respectively (Fig. 5d). Vertical profiles of RP in fall and spring were similar to those of ammonium concentration (data not shown), with a peak at the subsurface layer at a few stations. IRP in the UB was 127–434, 68–128, and 80–222 mg N m^{-2} d^{-1} in summer, fall, and spring, respectively (Table 1), exhibiting no significant seasonal variation (Kruskal-Wallis test, $p=0.070$).

4. Discussion

An interesting feature in spatial distribution of PP in the study area in summer is that IPP greatly increased along the northward pathway of the TWC system from the WPO through the ECS to the EJS. Summer IPP in the UB was about 2–3 times higher than those in the WPO and the ECS. Because it is widely accepted that PP in summer is lower than in spring or fall in temperate oceans, high PP in summer in the UB is abnormal. Previous reports also showed that the SW EJS had higher IPP than the WPO and offshore ECS (Shim and Park, 1986; Chung et al., 1989; Falkowski and Wilson, 1992; Chen, 1996; Hama et al., 1997; Gong et al., 2000; Chen and Chen, 2006; Hyun et al., 2009). Annual primary production is high (222 g C m^{-2} y^{-1}) in the UB (Yamada et al., 2005) compared the values (144–155 g C m^{-2} y^{-1}) in the subtropical WPO and the offshore ECS (Gong et al., 2000; Behrenfeld et al., 2006).

It is agreed upon that nutrient supply is the main key for the observed high IPP in the UB (see Shim and Park, 1986; Lee et al., 2009). However, mechanisms of nutrient supply are not well understood. Because nutrient supply to the UB from the Korean peninsula along the pathway is limited (Yoo and Park, 2009), other mechanisms need to be invoked. It was suggested that the northward flowing TWC and the East Korean Warm Current transport nutrient-rich water originating from upwelling on the southeast coast of Korea, enhancing primary production in the UB (Onitsuka et al., 2007; Hyun et al., 2009; Yoo and Park, 2009). However, upon examination of the satellite-SST, the affected area of cold SST was restricted to the coast and relatively narrow current streams (Yoo and Park, 2009). In our study period, the increase of surface PP due to nutrient-rich water supply by the upwelling was confined to Station C1, and features of the upwelling were not observed at Stations C2 and U1 located in the expected pathway of upwelled water and at other stations in the UB. Furthermore, IPP in the mixed layer (IPP_{ML}) at locations where the upwelled water is presumed to occupy, accounted for only $<$20% of the IPP (Table 1).

PP beneath the surface mixed layer accounted for the majority of IPP in the UB (Fig. 3). The high PP at the subsurface layer is believed to be related to shallowing of the pycnocline and thereby positioning of nutrient-replete water within the euphotic zone. In

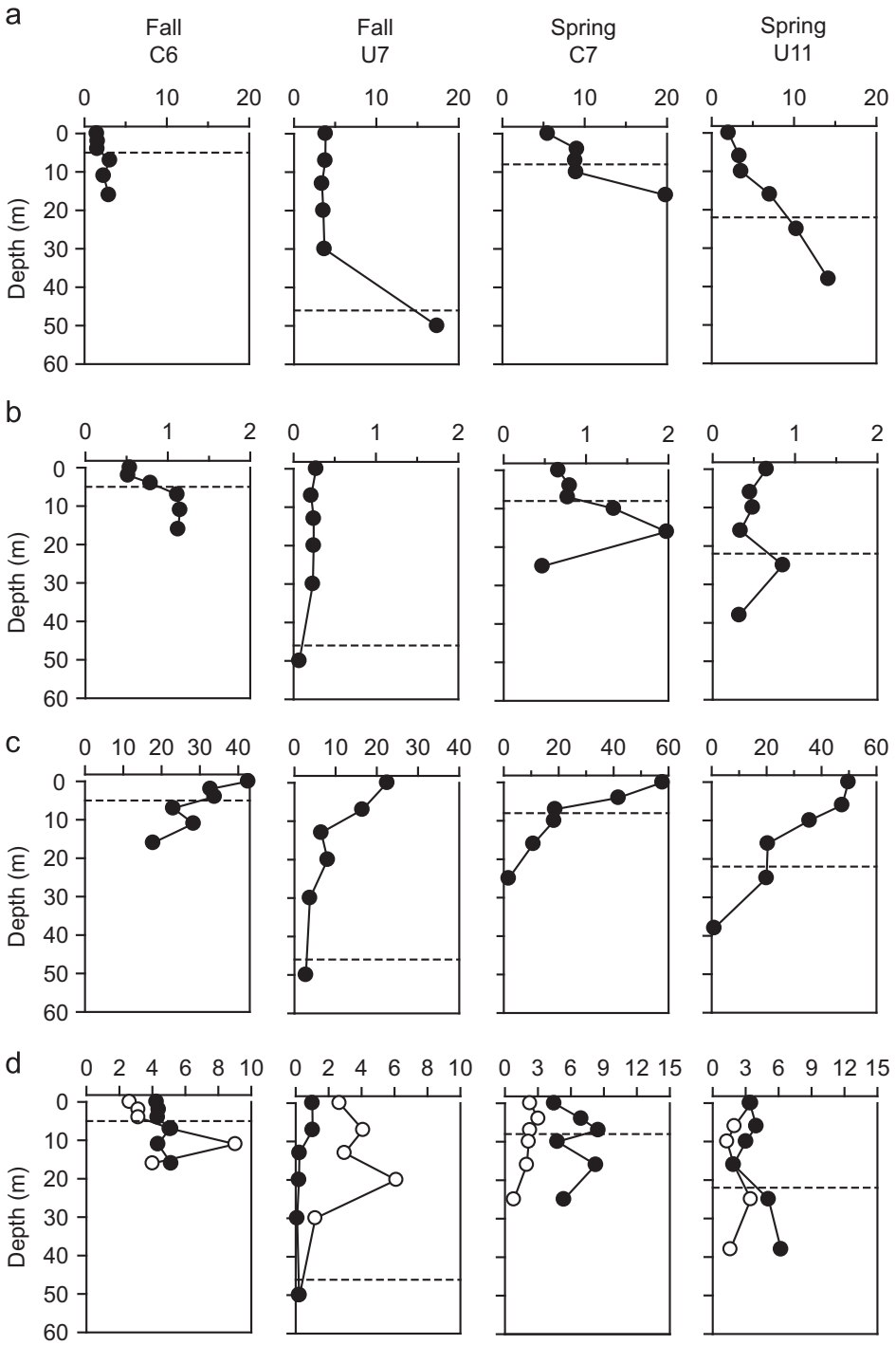

Fig. 5. Vertical profiles of (a) nitrate, (b) chlorophyll *a* concentration, (c) primary productivity (PP), (d) new productivity (NP, closed circles) and regenerated productivity (RP, open circles) in fall and in spring. Horizontal dashed lines represent the depth of the surface mixed layer.

addition, PP and NP in the mixed layer of the UB constituted low proportions of IPP and INP but were relatively high compared to the WPO and the ECS. Vertical advection and diffusion are expected to be an important source of nitrate to the mixed layer. We used the nitrate upward flux (F_n) at the bottom of the mixed layer as a qualitative indicator of nitrate supply to the mixed layer. Horizontal advection may also supply nutrients. However, estimation of the nitrate flux by horizontal advection was not possible because of the lack of spatial gradient in nitrate concentration. Nutrients in the TWC entering the EJS, were already depleted. Therefore, this source of nitrate may be small compared to the vertical supply. It is plausible that the sheer generated by the strong flow of the TWC may enhance the vertical supply of nitrate into the mixed layer. We expect that the eddy diffusivity originally obtained from the eastern tropical Pacific was probably smaller than the actual value in the UB. In this sense, the usage of the nitrate upward flux hence estimated should be considered as a conceptual model for future validation by more rigorous estimation of the eddy diffusivity in the study region. Although it can be important in the oligotrophic ocean, production based on N_2 fixation in the Kuroshio and the South China Sea was reported to be very low (Chen et al., 2008) compared to our new productivity

results. The nitrate upward flux at the bottom of the mixed layer in the EJS was higher than those in the ECS and the WPO (Table 2). Nitrate uptake rate in the mixed layer (Q_n) was strongly correlated with F_n in summer (Fig. 6a), clearly suggesting that the supply of nitrate from the underlying water enhanced primary production in the mixed layer. Therefore, it appears that shallowing of the pycnocline, and consequent positioning of the nutrient-replete water beneath the mixed layer facilitates high upward flux of nutrients. Consequent increase in PP in the mixed layer and at the SCM depth seems most likely process for the enhancement of IPP in summer in the UB. Indeed, the subsurface maximum PP, NP and chlorophyll *a* concentration that are closely associated with the nitracline immediately below the mixed layer further support this interpretation. In relation to the vertical distribution of chlorophyll *a*, SCM is commonly observed in marine environments characterized by a strong vertical stability (Furuya, 1990). Our study also demonstrates that spatial and seasonal variation of integrated chlorophyll *a* concentration over the euphotic zone showed a significant positive correlation with the stability index and an exponential correlation with the depth of the mixed layer, with the exception of the data at Stations C1 and C5 (Fig. 7a) and Stations C5 and C6 (Fig. 7b). This correlation implies that the SCM is likely supported by the nutrients supplied from below the nitracline (cf. Longhurst and Harrison, 1989).

Table 2
The diffusion coefficient (K_z), nitrate gradient ($\Delta NO_3^-/\Delta Z$), the upward flux of nitrate at the bottom of the mixed layer (F_n), and nitrate uptake rate in the mixed layer (Q_n) in summer.

Station	K_z ($cm^2\ s^{-1}$)	$\Delta NO_3^-/\Delta Z$ ($mmol\ m^{-4}$)	F_n ($\mu mol\ NO_3\ m^{-2}\ h^{-1}$)	Q_n ($\mu mol\ NO_3\ m^{-2}\ h^{-1}$)
WPO1	0.21	0.00	19	16
WPO2	4.46	0.01	31	36
ECS-S	0.37	0.02	1	1
ECS-N	3.27	0.24	3	1
C1	1.58	1.50	851	1220
C2	0.20	1.52	106	124
C3	0.37	0.62	83	65
C4	0.59	0.64	135	216
C5	0.53	0.35	66	40
U1	0.79	0.32	90	111
U2	0.42	0.42	64	117
U3	0.51	0.15	28	42
U4	0.15	0.08	4	4
U5	0.35	0.22	28	19

In the study area, the ratio of carbon to nitrogen uptake rates varied from 0.2 to 19.6 in summer (Appendix A). In most cases, the C:N uptake ratios were lower than the Redfield ratio (6.6). One possibility is that NP and RP may be overestimated due to the addition of $^{15}NO_3^-$ and $^{15}NH_4^+$ to the incubated samples, particularly in oligotrophic waters such as the WPO and the ECS stations (Hung et al., 2000; L'Helguen et al., 2002). However, the ratios were lower than the Redfield ratio even under nitrate-replete

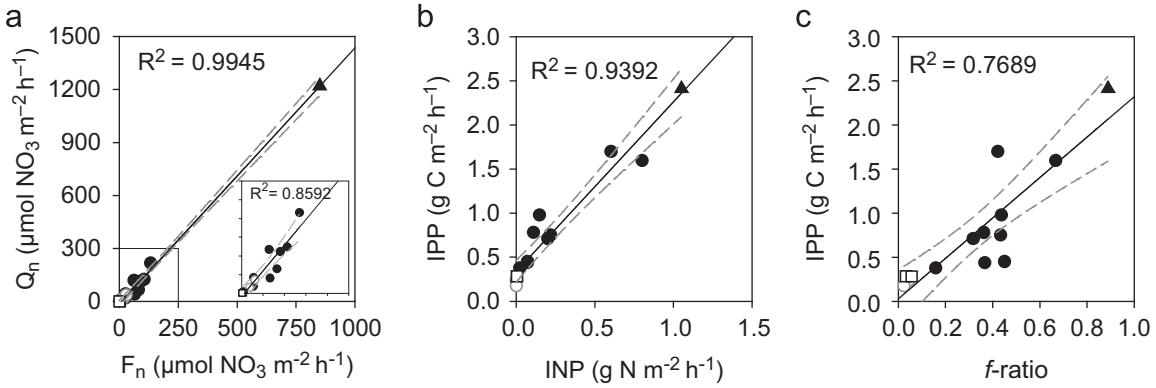

Fig. 6. Relationship between (a) nitrate upward flux (F_n) and integrated nitrate uptake in the surface mixed layer (Q_n), (b) IPP and INP, and (c) IPP and *f*-ratio in summer in the WPO (closed squares), the ECS (open circles), the UB (closed circles), and at the upwelling station (closed triangle). Solid lines and gray dashed lines represent regressions and 95% confidence intervals, respectively.

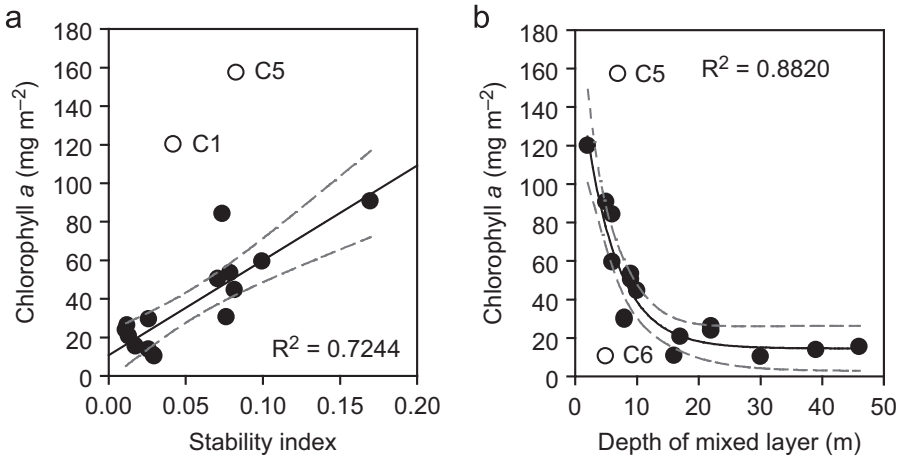

Fig. 7. (a) Linear correlation between integrated chlorophyll *a* concentration over the euphotic zone and stability index and (b) exponential correlation between integrated chlorophyll *a* over the euphotic zone and the depth of the mixed layer in the UB. Solid lines and gray dashed lines represent regressions and 95% confidence intervals, respectively.

condition of the UB. This suggests that the low C:N uptake ratio was not a methodological artefact but reflected a natural phenomenon caused by factors such as light and nitrate levels. In addition, phytoplankton assemblage and physiological status may also affect C:N uptake ratio (Banse 1994; Suárez and Marañón, 2003). Previous studies showed that C:N uptake ratios did not always correspond to C:N composition ratios of the particulate matter (Slawyk, 1979; Metzler et al., 1997; Hung et al., 2000). Hung et al. (2000) measured IPP and INP using ^{14}C and ^{15}N methods with the correction by nitrate reductase activity in the ECS and reported the depth-integrated C:N uptake ratios of 2.0–6.5 within the euphotic zone, showing much lower ratios in nitrate-replete waters and slightly lower in light-deficient waters than the Redfield ratio. A large variation of 0.1–25.1 in the C:N uptake ratios has also been reported in the Indian Ocean, decreasing with decreasing available radiation (Slawyk, 1979). Metzler et al. (1997) also found an extremely broad range of C:N uptake ratios (0.04–150) at the highly stratified shelf in the South Atlantic Ocean off Brazil. They observed that enhanced nitrogen uptake associated with the supply of nitrate led to the low ratio (0.04) at the bottom (1% of surface light intensity) of the euphotic zone. The low C:N uptake ratios obtained in the study area were consistent with these results.

We propose a conceptual model to explain the observed spatial variability in PP along the pathway of the TWC, based on a hypothesis that the high PP in the UB is supported by high nutrient (in particular, nitrate) availability in the euphotic zone, which is facilitated by hydrographic conditions (Fig. 8). Density at stations in the WPO and Station ECS-S increases gradually with increasing depth. This gradual increase expands well below the bottom of the euphotic zone. Nutrient concentrations, represented by nitrate, were uniformly low to a depth of 100 m or deeper. Hence, nutrient supply from the deeper waters to the euphotic zone is limited. As the surface current progresses through the ECS and enters the EJS, the pycnocline depth shallows dramatically as the warm water flows over the denser and colder ESPW that is replete with nutrients (Chang et al., 2004; Lee et al., 2009; references therein). As a result, strong stratification develops in shallow subsurface layer. The abundant nutrients immediately below pycnocline can be supplied into the mixed layer and also stimulate PP.

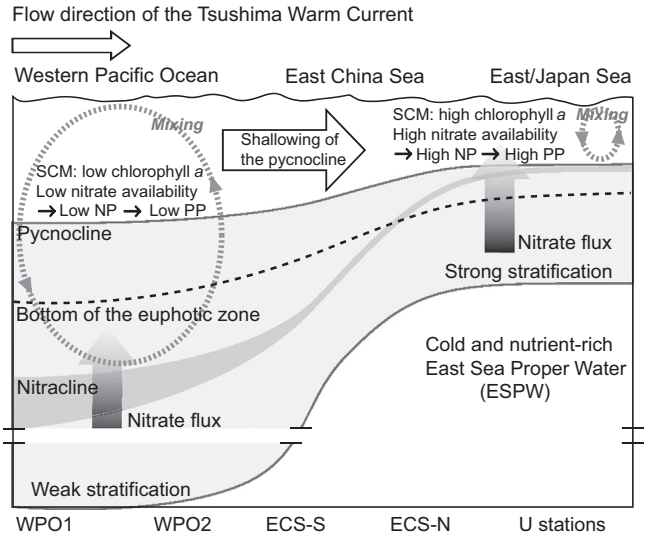

Fig. 8. A cartoon showing physicochemical and biological factors in the TWC system from the WPO to the EJS. SCM, subsurface chlorophyll maximum; PP, primary productivity; NP, new productivity.

We further compare the production-related parameters in fall and the following spring to better understand the summer time abnormality in the EJS. Although observations in fall and spring were not made at exactly the same stations as those in summer, they were within a good proximity for comparison for seasonal variability. Vertical structure of PP was quite different from summer through fall to spring with varying water column stability and vertical distributions of nutrient and chlorophyll *a* concentrations. In fall, the INP and the *f*-ratio were lower than those in summer and spring along with an increase in standing stock of ammonium (data not shown), while total nitrate in fall and spring showed a similar range to that in summer. This result suggests that the deepened surface mixed layer and the nitracline probably lowered nitrate availability in the euphotic zone in fall (Eppley and Peterson, 1979; Harrison et al., 1987). It has been generally accepted that phytoplankton prefer ammonium over other forms of nitrogen sources (Conway, 1977; McCarthy et al., 1977; Syrett, 1981; Glibert et al., 1982a). Ammonium concentration may control nitrate utilization by phytoplankton since a small relative increase in ammonium concentration can result in a dramatic reduction in the *f*-ratio (Murray et al., 1989; Wheeler and Kokkinakis, 1990; Peña et al., 1992). In spring, nitrate concentration increased sharply in the upper euphotic zone, while the standing stock of ammonium decreased. Such a vertical distribution of nitrate suggests that strong mixing replenished nitrate in the euphotic zone. This nutrient dynamics seems to explain the increase of the INP (also the *f*-ratio) in spring. High PP and low nitrate concentration in the surface water implies that the replenished nitrate is effectively utilized for primary production enhancing high surface PP, and further, to sustain high spring IPP.

A typical seasonal variation in IPP for a sea in the temperate zone (i.e. low primary productivity in summer rather than in spring and fall) was not observed in the UB. The seasonal variation in PP in the UB is not consistent with satellite-derived pattern in the UB (Yamada et al., 2005). In contrast to the subsurface maximum in summer 2008, PP was highest at the surface in fall 2008 and spring 2009. While summer PP and chlorophyll *a* concentration at the surface layer were lower than those in fall and spring, summer values at the subsurface layer were comparable to those in the surface water in fall and spring. These results show that high IPP in summer was mainly maintained by high PP at the SCM depth. This has implication in estimation of PP based on satellite observation: primary production based on satellite-based data (i.e. surface temperature and chlorophyll *a* concentration) could be largely underestimated in the UB especially in summer. For example, the mean of summer IPP in the UB (about 600 mg C m^{-2} d^{-1}) was about 1.5 times higher than a previous estimate (about 400 mg C m^{-2} d^{-1}) by Yamada et al. (2005).

5. Summary

A few interesting features are revealed from examination of hydrographic, chemical and biological parameters along the pathway of warm surface water of TWC system from the source region in the WPO through the ECS to the EJS. Primary productivity in the EJS is significantly higher than that in the upstream of the TWC system. As the TWC flows over a colder and denser water mass in the southwest EJS, the bottom of the pycnocline and the surface mixed layer become shallower to be located above the euphotic depth. In the EJS, the observed high PP and NP at the SCM depth are believed to be sustained by shallowing of the pycnocline and thereby positioning of nutrient-rich water within the euphotic zone. The high productivities in the mixed layer and at the SCM depths were supported by an upward flux of nutrients across the pycnocline to the mixed layer (Fig. 8). High nitrate availability due

to such a hydrographic feature in summer can be an important mechanism for high PP in the UB in addition to an existing hypothesis of upwelling-derived enhancement of PP. PP in the UB in summer was not significantly lower than those in spring and fall. The high PP is believed to be sustained by a subsurface maximum of chlorophyll *a* and PP. Our summer data also imply that IPP estimation by satellite-based chlorophyll *a* data needs to be interpreted with caution in the regions of similar hydrographic features as in the EJS.

Acknowledgments

We would like to thank Dr. C.-W. Shin for shared ship time, and the captains and crews of R/Vs Onnuri, Haeyang 2000, Eardo, and Tamyang. This research was carried out as a part of the project titled 'East Asian Seas Time series-I (EAST-I)', funded by the Ministry of Oceans and Fisheries, Korea.

Appendix A. Supplementary information

Supplementary data associated with this article can be found in the online version at http://dx.doi.org/10.1016/j.dsr.2013.05.011.

References

Banse, K., 1994. Uptake of inorganic carbon and nitrate by marine plankton and the Redfield ratio. Global Biogeochem. Cycles 8, 81–84.
Behrenfeld, M.J., Worthington, K., Sherrell, R.M., Chavez, F.P., Strutton, P., 2006. Controls on tropical Pacific Ocean productivity revealed through nutrient stress diagnostics. Nature 442, 1025–1028.
Bode, A., Castro, C.G., Doval, M.D., Varela, M., 2002. New and regenerated production and ammonium regeneration in the western Bransfield Strait region (Antarctica) during phytoplankton bloom conditions in summer. Deep-Sea Res. II 49, 787–804.
Chang, K.-I., Teague, W.J., Lyu, S.J., Perkins, H.T., Lee, D.K., Watts, D.R., Kim, Y.B., Mitchell, D.A., Lee, C.M., Kim, K., 2004. Circulation and currents in the southwestern East/Japan Sea: Overview and review. Prog. Oceanogr. 61, 105–156.
Chen, C.T.A., 1996. The Kuroshio intermediate water is the major source of nutrients on the East China Sea continental shelf. Oceanolog. Acta 19, 523–527.
Chen, Y.L., Lu, H.B., Shiah, F.K., Gong, G.C., Liu, K.K., Kanda, J., 1999. New production and *f*-ratio on the continental shelf of the East China Sea: Comparisons between nitrate inputs from the subsurface Kuroshio Current and the Changjiang River. Estuarine Coastal Shelf Sci. 48, 59–75.
Chen, Y.L., Chen, H.Y., Lee, W.H., Hung, C.C., Lee, W.H., Hung, Wong, G.T.F., Kanda, J., 2001. New production in the East China Sea, comparison between well-mixed winter and stratified summer conditions. Cont. Shelf Res. 21, 751–764.
Chen, Y.L., Chen, H.Y., 2006. Seasonal dynamics of primary production and new production in the northern South China Sea: the significance of river discharge and nutrient advection. Deep-Sea Res. I 53, 971–986.
Chen, Y.L., Chen, H.Y., Tuo, S.H., Ohki, K., 2008. Seasonal dynamics of new production from *Trichodesmium* N_2 fixation and nitrate uptake in the upstream Kuroshio and South China Sea basin. Limnol. Oceanogr. 53, 1705–1721.
Cho, B.C., Park, M.G., Shim, J.H., Choi, D.H., 2001. Sea-surface temperature and *f*-ratio explain large variability in the ratio of bacterial production to primary production in the Yellow Sea. Mar. Ecol. Prog. Ser. 216, 31–41.
Chung, C.S., Shim, J.H., Park, Y.C., Park, S.G., 1989. Primary productivity and nitrogenous nutrient dynamics in the East Sea of Korea. J. Oceanol. Soc. Korea 24, 52–61.
Conway, H.L., 1977. Interactions of inorganic nitrogen in the uptake and assimilation by marine phytoplankton. Mar. Biol. 39, 221–232.
Dore, J.E., Letelier, R.M., church, M.J., Lukas, R., Karl, D.M., 2008. Summer phytoplankton blooms in the oligotrophic North Pacific Subtropical Gyre: historical perspective and recent observations. Prog. Oceanogr. 76, 2–38.
Dugdale, R.C., Goering, J.J., 1967. Uptake of new and regenerated forms of nitrogen in primary productivity. Limnol. Oceanogr. 12, 196–206.
Dugdale, R.C., Wilkerson, F.P., 1986. The use of ^{15}N to measure nitrogen uptake in eutrophic ocean; experimental considerations. Limnol. Oceanogr. 31, 673–689.
Dugdale, R.C., Wilkerson, F.P., Barber, R.T., Chavez, F.P., 1992. Estimating new production in the equatorial Pacific Ocean at 150°W. J. Geophys. Res. 97, 681–686.
Edmond, J.M., Gieskes, J.M., 1970. On the calculation of the degree of saturation of sea water with respect to calcium carbonate under in situ conditions. Geochim. Cosmochim. Acta 34, 1261–1291.
Eppley, R.W., Peterson, B.J., 1979. Particulate organic matter flux and planktonic new production in the deep ocean. Nature 282, 677–680.
Eppley, R.W., Renger, E.H., Harrison, G., 1979. Nitrate and phytoplankton production in southern California coastal waters. Limnol. Oceanogr. 24, 483–494.
Falkowski, P.G., Wilson, C., 1992. Phytoplankton productivity in the North Pacific Ocean since 1900 and implications for absorption of anthropogenic CO_2. Nature 358, 741–743.
Fan, C., Glibert, P.M., 2005. Effects of light on nitrogen and carbon uptake during a *Prorocentrum minimum* bloom. Harmful Algae 4, 629–641.
Furuya, K., 1990. Subsurface chlorophyll maximum in the tropical and subtropical western Pacific Ocean: vertical profiles of phytoplankton biomass and its relationship with chlorophyll *a* and particulate organic carbon. Mar. Biol. 107, 529–539.
Glibert, P.M., Biggs, D.C., McCarthy, J.J., 1982a. Utilization of ammonium and nitrate during austral summer in the Scotia Sea. Deep-Sea Res. I 29, 837–850.
Glibert, P.M., Lipschultz, F., McCarthy, J.J., Altabet, M.A., 1982b. Isotope dilution models of uptake and remineralization of ammonium by marine plankton. Limnol. Oceanogr. 27, 639–650.
Gong, G.C., Shiah, F.K., Liu, K.K., Wen, Y.H., Liang, M.H., 2000. Spatial and temporal variation of chlorophyll *a*, primary productivity and chemical hydrography in the southern East China Sea. Cont. Shelf Res. 20, 411–436.
Hama, T., Miyazaki, T., Ogawa, Y., Iwakuma, M., Takahashim, M., Otsuki, A., Ichimura, S., 1983. Measurement of photosynthetic production of a marine phytoplankton population using a stable isotope ^{13}C isotope. Mar. Biol. 73, 31–36.
Hama, T., Shin, K.H., Handa, N., 1997. Spatial variability in the primary productivity in the East China Sea and its adjacent waters. J. Oceanogr. 53, 41–51.
Harrison, W.G., Platt, T., Lewis, M.R., 1987. *f*-Ratio and its relationship to ambient nitrate concentration in coastal waters. J. Plankton Res. 9, 235–248.
Howarth, R.W., Marino, R., Cole, J.J., 1988. Nitrogen fixation in freshwater, estuarine, and marine ecosystems. 1. Rates and importance. Limnol. Oceanogr. 33, 669–687.
Hung, C.C., Wong, G.T.F., Liu, K.K., Shiah, F.K., Gong, G.C., 2000. The effect of light and nitrate levels on the relationship between nitrate reductase activity and $^{15}NO_3^-$ uptake: field observations in the East China Sea. Limnol. Oceanogr. 45, 836–848.
Hyun, J.H., Kim, D., Shin, C.W., Noh, J.H., Yang, E.J., Mok, J.S., Kim, S.H., Kim, H.C., Yoo, S., 2009. Enhanced phytoplankton and bacterioplankton production coupled to coastal upwelling and an anticyclonic eddy in the Ulleung Basin, East Sea. Aquat. Microb. Ecol. 54, 45–54.
Isoda, Y., Saitoh, S.I., 1993. The northward intruding eddy along the East Coast of Korea. J. Oceanogr. 49, 443–458.
Kanda, J., Saino, T., Hattori, A., 1985. Nitrogen uptake by natural populations of phytoplankton and primary production in the Pacific Ocean: regional variability of uptake capacity. Limnol. Oceanogr. 30, 987–999.
Kanda, J., Laws, E.A., Saino, T., Hattori, A., 1987. An evaluation of isotope dilution effect from conventional data sets of ^{15}N uptake experiments. Journal of Plankton Research 9, 79–90.
King, F.D., Devol, A.H., 1979. Estimates of vertical eddy diffusion through the thermocline from phytoplankton nitrate uptake rates in the mixed layer of the eastern tropical Pacific. Limnol. Oceanogr. 24, 645–651.
L'Helguen, S., Corre, P.L., Madec, C., Morin, P., 2002. New and regenerated production in the Almeria-Oran front area, eastern Alboran Sea. Deep-Sea Res. I 49, 83–99.
Lee, J.C., 1983. Variations of sea level and sea surface temperature associated with wind-induced upwelling in the southeast coast of Korea in summer. J. Oceanol. Soc. Korea 18, 149–160.
Lee, J.C., Na, J.Y., 1985. Structure of upwelling off the southeast coast of Korea. J. Korean Soc. Oceanogr. 20, 6–19.
Lee, J.Y., Kang, D.J., Kim, I.N., Rho, T., Lee, T., Kang, C.K., Kim, K.R., 2009. Spatial and temporal variability in the pelagic ecosystem of the East Sea (Sea of Japan): a review. J. Mar. Syst. 78, 288–300.
Longhurst, A.R., Harrison, W.G., 1989. The biological pump: profiles of plankton production and consumption in the upper ocean. Prog. Oceanogr. 22, 47–123.
Marty, J.C., Garcia, N., Raimbault, P., 2008. Phytoplankton dynamics and primary production under late summer conditions in the NW Mediterranean Sea. Deep-Sea Res. I 55, 1131–1149.
McCarthy, J.J., Taylor, W.R., Taft, J.L., 1977. Nitrogenous nutrition of the plankton in the Chesapeake Bay. 1. Nutrient availability and phytoplankton preferences. Limnol. Oceanogr. 22, 996–1011.
McCarthy, J.J., Garside, C., Nevins, J.L., Barber, R.T., 1996. New production along 140°W in the equatorial Pacific during and following the 1992 El Nino event. Deep-Sea Res. II 43, 1065–1093.
Metzler, P.M., Glibert, P.M., Gaeta, S.A., Ludlam, J.M., 1997. New and regenerated production in the South Atlantic off Brazil. Deep-Sea Res. I 44, 363–384.
Murray, J.W., Downs, J.N., Strom, S., Wei, C.L.., Jannasch, H.W., 1989. Nutrient assimilation, export production and 234Th scavenging in the eastern equatorial Pacific. Deep Sea Res. 36, 1471–1489.
Onitsuka, G., Yanagi, T., Yoon, J.H., 2007. A numerical study on nutrient sources in the surface layer of the Japan Sea using a coupled physical-ecosystem model. J. Geophys. Res. 112, C05042, http://dx.doi.org/10.1029/2006JC003981.
Parker, A.E., Wilkerson, F.P., Dugale, R.C., Marchi, A.M., Hogue, V.E., Landry, M.R., Taylor, A.G., 2011. Spatial patterns of nitrogen uptake and phytoplankton in the equatorial upwelling zone (110°W–140°W) during 2004 and 2005. Deep-Sea Res. II 58, 417–433.
Parsons, T.R., Maita, Y., Lalli, C.M., 1984. A Manual of Chemical and Biological Methods for Seawater and Analysis. Pergamon Press Oxford, p. 173.
Peña, M.A., Harrison, W.G., Lewis, M.R., 1992. New production in the central equatorial Pacific. Mar. Ecol. Prog. Ser. 80, 265–274.

Shim, J.H., Park, Y.C., 1986. Primary productivity Measurement using carbon-14 and nitrogenous nutrient dynamics in the southeastern sea of Korea. J. Oceanol. Soc. Korea 21, 13–24.
Shin, H.R., Kim, C.W., Byun, S.K., Hwang, S.C., 2005. Movement and structural variation of warm eddy WE92 for three years in the western East/Japan Sea. Deep-Sea Res. II 52, 1742–1762.
Slawyk, G., 1979. ^{13}C and ^{15}N uptake by phytoplankton in the Antarctic upwelling area: results from the Antiprod I Cruise in the Indian Ocean sector. Aust. J. Mar. Freshwater Res. 30, 431–448.
Suárez, I., Marañón, E., 2003. Photosynthate allocation in a temperate sea over an annual cycle: the relationship between protein synthesis and phytoplankton physiological state. J. Sea Res. 50, 285–299.
Sverdrup, H.U., 1953. On conditions for the vernal blooming of phytoplankton. Journal du Conseil, Conseil permanent international pour l'exploration de la mer 18, 287–295.
Syrett, P.J., 1981. Nitrogen metabolism of microalgae. Can. Bull. Fish. Aquat. Sci. 210, 182–210.
Vitousek, P.M., Howarth, R.W., 1991. Nitrogen limitation on land and in the sea: how can it occur? Biogeochemistry 13, 87–115.
Wheeler, P.A., Kokkinakis, S.A., 1990. Ammonium recycling limits nitrate use in the oceanic subarctic Pacific. Limnol. Oceanogr. 35, 1267–1278.
Wilson, C., Villareal, T.A., Maximenko, N., Bograd, S.J., Montoya, J.P., Schoenbaechler, C.A., 2008. Biological and physical forcings of late summer chlorophyll blooms at 30°N in the oligotrophic Pacific. J. Mar. Syst. 69, 164–176.
Yamada, K., Ishizaka, J., Nagata, H., 2005. Spatial and temporal variability of satellite primary production in the Japan Sea from 1998 to 2002. J. Oceanogr. 61, 857–869.
Yoo, S., Park, J., 2009. Why is the southwest the most productive region of the East Sea/Sea of Japan? J. Mar. Syst. 78, 301–315.